

Design of Compact Bandpass Filters based on Fractal Defected Ground Structure (DGS) Resonators

Jawad K. Ali* and Hadi T. Ziboon

Microwave Research Group, Department of Electrical Engineering, University of Technology, Baghdad, Iraq; jawadkali@theiet.org, haditarishziboon@yahoo.co.uk

Abstract

Modified Minkowski fractal geometry has been found to be attractive for microwave circuit designers because of its high space-filling property. This property will lead to the design of compact circuits; meeting the requirements of the modern communications systems to be with small size. In this paper, the design of a compact microstrip BandPass Filters (BPF) has been proposed based on the modified Minkowski fractal (DGS) resonators. The proposed BPF structure is composed of two coupled resonators etched as fractal DGS structures. Results reveal that as the iteration level of fractal based DGS becomes higher, more compact filter structure will result in. Furthermore, the presented DGS structures with fractal-shaped resonators can be adopted to design compact planar BPFs with reasonable performances. The performance curves offered by the resulting filters are characterized by the low loss across the passband and high rejection levels outside it with steep roll-off in both edges of passband. Measured results of a fabricated prototype of a 2nd iteration fractal DGS BPF have shown reasonable agreement with those predicted by simulation. Measured results of a 2nd iteration fractal DGS BPF have shown satisfactory agreement as compared with simulation results. There is a slight shift of the lower edge of the passband response of the transmission characteristics, while the upper edge is very close. The results have shown that the filter has reasonable performance characteristics with considerable reduction of higher harmonics. The compact size of the proposed filter together with the realized high selectivity will make it suitable for a broad range of the recently available wireless communication services.

Keywords: Compact Bandpass Filter; Fractal-based BPF; Defected Ground Structure; Electromagnetic Modeling and Simulation; Minkowski Fractal Geometry

1. Introduction

Various fractal geometries are characterized by two unique properties; space-filling and self-similarity. These properties have opened new and essential approaches for antennas and electronic solutions in the course of the most recent 25 years. This preliminary stage gives a prologue to the benefits given by fractal geometry in antennas, resonators, and related structures. Such profits incorporate, among numerous, wider bandwidths, littler sizes, part-less electronic parts, and better performance. Additionally, fractals give another era of optimized design tools, initially utilized effectively in antennas but applicable in a general manner¹.

In the antenna design, the unique properties of space-filling and self-similarity that different fractal geometries possess were successfully employed to produce miniaturized multiband radiating structures²⁻⁹. Furthermore, various fractal curves were suggested to be applied to the traditional microstrip resonators which are successfully adopted to design miniaturized antennas and filters for a wide range of communication applications. Based on the traditional square patch, Sierpinski carpet has been employed to construct a dual-mode microstrip bandpass filter^{10,11}. Furthermore, many conventional fractal geometries have also found their way in the design compact BPF structures^{12,13}. The Peano fractal geometry and its variants have been used in the traditional

* Author for correspondence

resonators to produce successful high-performance compact size single and dual-mode microstrip bandpass filters^{14–17}. The high space-filling property of this fractal geometry makes it an attractive choice to design bandpass filters with high size reduction levels. The high space-filling property of the Minkowski fractal based microstrip resonators has more attracted microwave filter designers to successfully suggest them to design miniaturized dual-mode fractal based microstrip ring resonator BPFs^{18–21}. Also, Minkowski Island has been adopted to create a hairpin BPF with harmonic suppression²².

On the other hand, the application of the DGS to produce compact size filter and better performance has shown to be interesting, and an increasing research work has been reported. Unfortunately, the majority of the published research has been devoted to the design of lowpass filter design. In this respect, the use of fractal geometries to modify the shapes of the DGS structures has shown effective to provide further miniaturization and enhanced LPFs and BPFs performance^{23–28}. A DGS in the form of Hilbert fractal Curve Ring (HCR) has been investigated to design a compact LPF²³. A DGS cell model in the form of HCR with open stubs loaded on the conductor line is adopted to improve the performance of the filter out-band suppression. A Sierpinski carpet fractal DGS is effectively applied to design a LPF in²⁴, where a simple structure and high-power handling capability are obtained from the proposed filter. Furthermore, Minkowski and Koch fractal geometries have been applied to form DGS complementary split ring resonators design miniaturized BPFs^{25,26}.

In this paper, a compact BPF with fractal based DGS resonators is presented. Minkowski fractal curve, with different iteration levels, were used to shape DGS structures of the suggested filter. Besides the miniaturized size, the resulting BPF has been shown to offer reasonable passband response with reduced higher harmonics. Although the employment of the different fractal geometries in the design of DGS resonators to construct compact planar BPFs, but the authors believe that the presented filter design over-performs many of its class in that it offers compact size together with reasonable passband characteristics as will be shown in the following sections.

2. The Filter Structure

The structure of the proposed microstrip BPF is considered as a modification of that adopting the traditional open-loop coupled rings and other Euclidean shaped DGS resonators, reported in the literature^{27,28}, as a starting step. In this work, the suggested DGS coupled resonators will take the shape of the Minkowski fractal geometries shown in Figure 1.

Essentially, the modification carried out to reshape the structures depicted in Figure 1 is a means to increase the length occupied by the fractal based resonator at resonance. Subsequently, this will result in an increase of the surface current path length which in turns leading to a reduced resonant frequency. Therefore, a compact size resonator will result in, if the design frequency is kept unchanged. The fractal-based perimeter P_n of the n th iteration structure, will be given by^{18,25}:

$$P_n = \left(1 + 2 \frac{w_2}{L_o}\right) P_{n-1} \quad (1)$$

where, w_2 and L_o are as outlined in Figure 1. Apparently,

as n increases, the resulting fractal perimeter will increase accordingly. The space-filling property of the fractal based structure to increase its length in the succeeding iterations was found very attractive for considering its size reduction ability as a BPF. In this paper, the proposed BPF structure is consist of two main parts; the first is a center slotted microstrip transmission line to be etched on one side of a substrate, while the other side of the substrate will constitute a modified Minkowski fractal based DGS. Different BPF structures will be examined corresponding to the different iteration levels.

3. The Proposed Filter Design

Many DGS microstrip BPFs have been modeled with their ground planes being defected by slot structures in the form of two coupled resonators. The proposed DGS structures are composed of two coupled open loop slot resonators based on the modified Minkowski fractal iteration levels; starting from zero iteration up to the 2nd iteration level as depicted in Figure 1. Three BPFs, each with different iteration fractal DGS structure will be modeled and their performance has to be evaluated using

the Method of Moments (MoM) based electromagnetic simulator, IE3D²⁹.



Figure 1. The steps of growth of the Minkowski-like pre-fractal structure: (a) the generator, (b) the square ring, (c) the 1st iteration, and (d) the 2nd iteration^{18,25}.

Figure 2 demonstrate the layout of the modeled filter with its ground plane being defected by two coupled open loop slots in the form of the 2nd iteration Minkowski fractal geometry. On the top of the substrate, a transmission line is etched with a gap having a width D is embedded in its center. The substrate has a relative dielectric constant of 2.65 and thickness of 1.0 mm. The input/output ports have 50Ω characteristic impedance. The corresponding transmission line will have a width of about 2.75 mm.

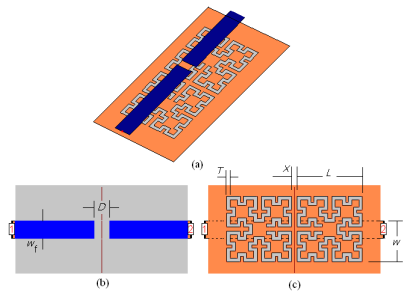


Figure 2. (a) The modeled fractal based DGS BPF configuration, (b) The top view and (c). The bottom view.

The side length, L , of the resonators of the modeled filters has been kept unchanged as that of the square open-loop. At the design frequency of 2.45 GHz, it has been found that the modeled BPF with zero iteration DGS resonates when L is equal to about 12.50 mm. This length represents about 0.15 the guided wavelength, λ_g . The guided wavelength is calculated as:

$$\lambda_g = \frac{\lambda_0}{\sqrt{\epsilon_{eff}}} \quad (2)$$

where, ϵ_{eff} is the effective dielectric constant. Many electromagnetic simulators permit the calculation of ϵ_{eff} using empirical expressions as reported in the literature^{29,30}. Nevertheless, applying fractal geometries implies that larger length has been included in the resonator structures which are not equal to half or multiple of λ_g at resonance, because not all the resonator

length will contribute to achieve resonance. This can be clearer when investigating the current distribution on the ground plane at resonance as will be shown later.

It is worth to note that the resonator side lengths of the modeled filters in this paper are maintained unchanged at this value. As will be shown later, the gap width, D , the inter-resonator spacing, X and the distance between the filter longitudinal center and the transmission line lower edge, W play important roles in the resulting filter performance.

4. Performance Evaluation

The performance of a BPF is typically evaluated throughout its passband characteristics, including passband insertion loss. It is required that the passband insertion loss should be as low as possible and consistently low as possible across the full passband. The BPF should provide as much rejection of unwanted signals as possible, both in its lower stopband and upper stopband outside of the low-loss passband. In this context, as a measure of the degree of selectivity of the BPF response, it can be described by what is known the roll-off rate^{31–33}. The roll-off rate, R , of a filter response is defined as:

$$R = \frac{|\alpha_{\max} - \alpha_{\min}|}{|f_s - f_c|} \quad (3)$$

where, α_{\max} is the 40 dB attenuation point and α_{\min} is the 3 dB attenuation point; f_s is the 40 dB stopband frequency and f_c is the 3 dB cutoff frequency. It is worth to note that, different values might be assigned to α_{\max} in order to determine the roll-off rate³⁴. However, in this work α_{\max} has been chosen to be 40 dB.

BPFs with the DGS structures as those depicted in Figure 3, have been modeled and analyzed using the commercially available EM simulator, IE3D. Two other filters have been designed; both with the fractal based resonators DGS as depicted in Figures 3(a) and 3(b).

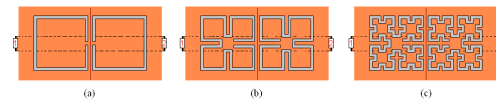


Figure 3. The bottom view of the modeled BPFs with: (a) zero iteration fractal DGS, (b) the 1st iteration fractal DGS, and (c) the 2nd iteration fractal DGS.

5. Parametric Study

Three BPFs with fractal based DGS structures depicted

in Figure 3(a), have been modeled and analyzed. The side length L of all the coupled DGS resonators of the modeled filters has been kept unchanged at 12.50 mm and slot trace width, T of about 0.61 mm. At this length, the zero iteration DGS BPF resonates at 2.50 GHz. A parametric study has been conducted to examine the influences of the various filter elements on its performance.

The effect of varying the gap width D , while keeping other parameters unchanged, has been shown in Figure 4. The increase of D leads to shift the transmission zeros away from the center frequency while almost has no effect on the passband. As D becomes larger, this will expand the filter bandwidth at the expense of reduction of the filter selectivity. At certain value of D , the upper transmission zero disappears. The effect of varying inter-resonator spacing X has been shown in Figure 5. In comparison with the effect of D , varying X will be slight on both the passband and stopband.

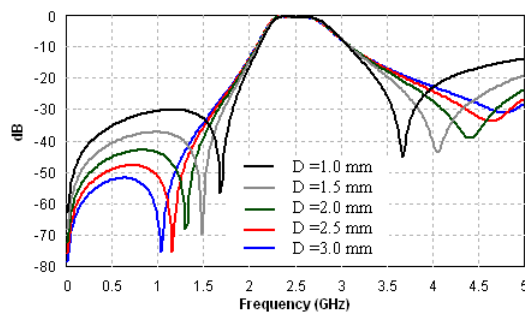


Figure 4. Simulated transmission responses of the zero iteration fractal DGS BPFs with $W=1.5$ mm, $X=2.5$ mm and D as a parameter.

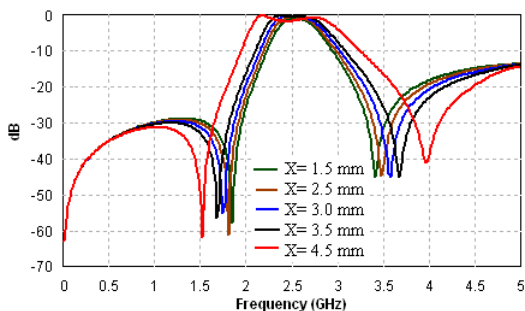


Figure 5. Simulated transmission responses of the zero iteration fractal DGS BPFs with $W=1.5$ mm, $D=2.5$ mm and X as a parameter.

Varying the feed line position, W , with respect to the filter longitudinal center has a significant effect as clearly shown in Figure 6. Both the filter passband and stopband are considerably deteriorated. As the feed line becomes near the DGS edge, the filter performance has been improved. Best performance has found at $W=1.5$ mm, $X=2.5$ mm and $D=1.0$ mm. This is depicted in Figure 7 which demonstrates the in-band and out-of-band filter reflection and transmission responses.

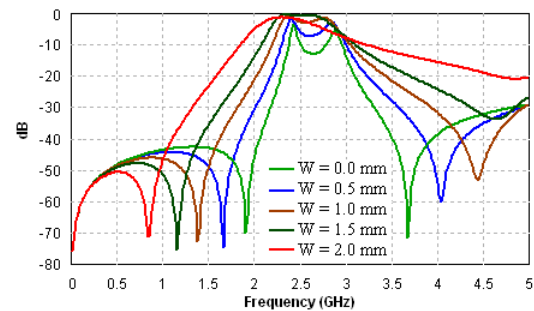


Figure 6. Simulated transmission responses of the zero iteration fractal DGS BPFs with $X=2.5$ mm, $D=2.5$ mm and W as a parameter.

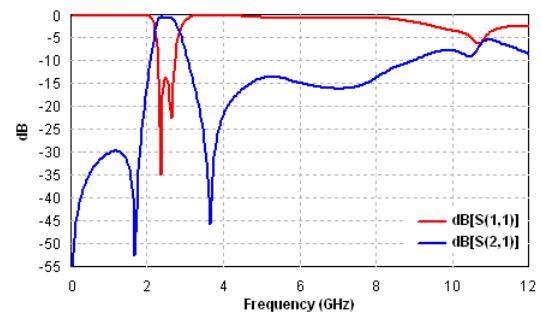


Figure 7. Simulated transmission and reflection coefficient responses of the zero iteration fractal DGS BPF with $W=1.5$ mm, $X=2.5$ mm and $D=1.0$ mm.

Similar parametric study has been carried out for the BPF with 1st iteration fractal DGS having the same resonator side length. The extra length provided by the 1st iteration fractal resonator, makes the filter resonating at a lower frequency. The resulting filter has a resonant frequency of about 1.61 GHz. Compared with the zero iteration fractal DGS BPF; this corresponds to a size reduction of about 65%.

Besides the size reduction, the 1st iteration fractal DGS BPF over performs that with zero iteration fractal DGS in that it offers better selectivity. The effects of varying the parameters; D , X , and W on the filter performance are depicted in Figures 8–10 respectively.

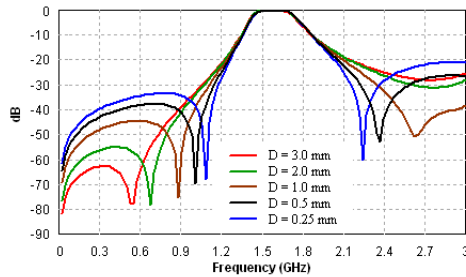


Figure 8. Simulated transmission responses of the 1st iteration fractal DGS BPFs with $W=2.25$ mm, $X=1.0$ mm and D as a parameter.

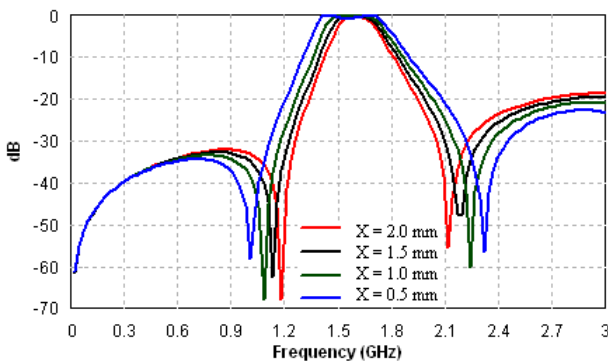


Figure 9. Simulated transmission responses of the 1st iteration fractal DGS BPF with $W=2.25$ mm, $D=0.25$ mm and X as a parameter.

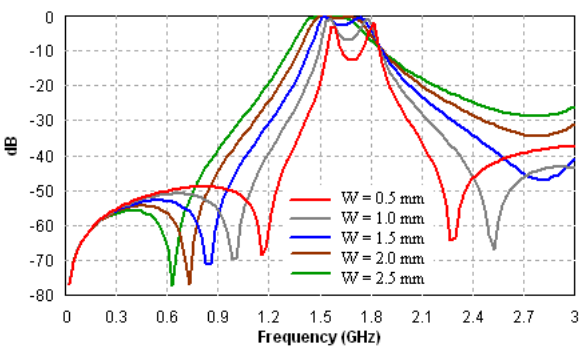


Figure 10. Simulated transmission responses of the 1st iteration fractal DGS BPFs with $X=1.0$ mm, $D=2.0$ mm and W as a parameter.

For this filter, best performance has found at $W=2.25$

mm, $X=2.0$ mm and $D=0.25$ mm. This is depicted in Figure 7 which demonstrates the in-band and out-of-band filter reflection and transmission responses.

From the results in Figure 11, the filter has a center frequency at 1.61 GHz with symmetrical response about the center frequency. The results imply that the filter offers two transmission zeros positioned at 1.33 GHz and 2.15 GHz. The filter has steeper response with higher roll-off rates of about 132.74 dB/GHz and 94.81 dB/GHz at the lower and the upper edges of the passband respectively. In addition, the filter has more rejection level in the stopband as compared with the 1st iteration fractal DGS BPF previously prescribed.

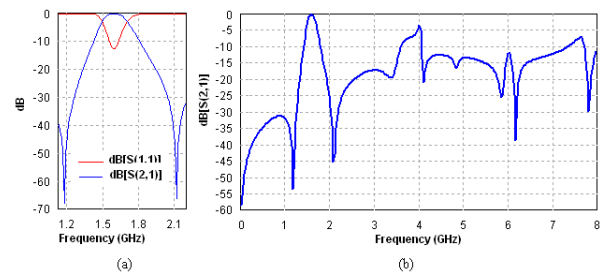


Figure 11. Simulated transmission and reflection coefficient responses of the 1st iteration fractal DGS BPF with $W=2.25$ mm, $X=2.0$ mm and $D=0.25$ mm; (a) The in-band response, and (b) The out-of-band response.

Bandpass filters based on the 2nd iteration fractal DGS are found the best among the investigated filters. Figures 12–14 demonstrate the filter performance responses under the effects of varying the parameters; D , X , and W . It is clear from the results that the BPF based on 2nd iteration fractal DGS than the other two filters in many respects. This filter offers the highest selectivity and the highest rejection level in the stopband.

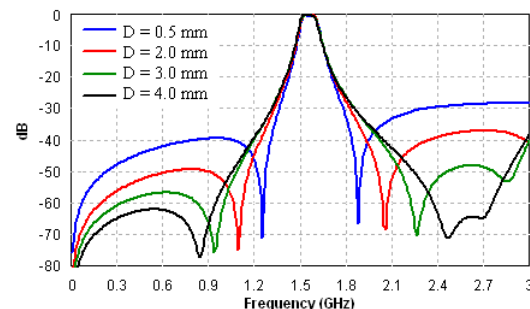


Figure 12. Simulated transmission responses of the 2nd iteration fractal DGS BPFs with $W=1.5$ mm, $X=4.0$ mm and D as a parameter.

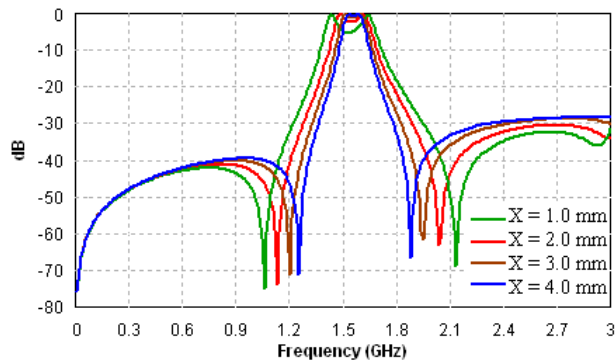


Figure 13. Simulated transmission responses of the 2nd iteration fractal DGS BPFs with $W=1.5$ mm, $D=1.0$ mm and X as a parameter.

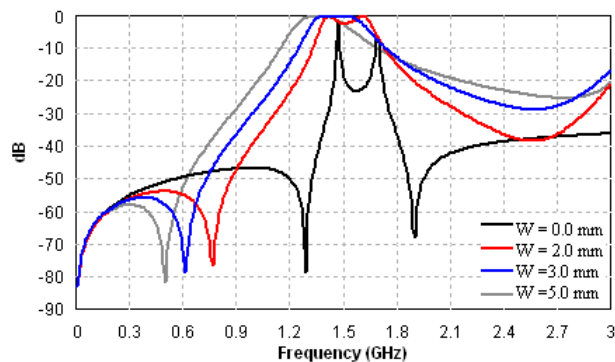


Figure 14. Simulated transmission responses of the 2nd iteration fractal DGS BPFs with $X=1.0$ mm, $D=2.0$ mm and W as a parameter.

Figure 15 demonstrates the responses of the resulting filter. As the results in Figure 15(a) imply, the filter possesses an in-band response with steep roll-off. The -40 dB lower edge roll-off rate of the passband is of about 197.70 dB/GHz, and that of the upper edge is of about 180.04 dB/GHz. It also has two transmission zeros that are almost symmetrically positioned about the center frequency and located at 1.32 GHz and 1.87 GHz. On other hand, Figure 15(b) shows the out-of-band filter response. It is clear that the filter doesn't support the higher harmonics which normally accompany the performance of BPFs. Furthermore, according to ^{19,20}, the positions of the transmission zeros is highly affected by the equivalent capacitance of the DGS structures. As the iteration level becomes higher of the successive structures while the side length maintained fixed, the included length becomes larger and substructures of the resonators become near each other; creating a capacitive coupling which in turns improves the resulting filter skirt characteristics at both

edges.

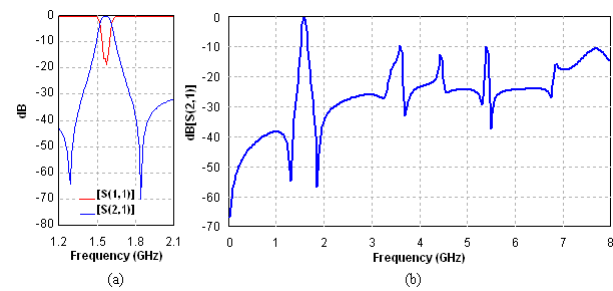


Figure 15. Simulated transmission and reflection coefficient responses of the 2nd iteration fractal DGS BPF with $W=1.5$ mm, $X=5.0$ mm and $D=1.0$ mm; (a). The in-band response and (b). The out-of-band response.

On the other hand, all of the presented filters in the article are of second order which means that they necessarily have two poles in their return loss responses. It is clear that the response of the Figure 7 has two poles while those of Figures 15 and 17 have one pole. This is because that the poles of the filter responses depicted in Figures 15 and 17 are very close and superimposed on each other and appear as if they possess one pole.

Moreover, to present more physical explanation about the EM aspects of the proposed filter, the simulated current distributions on its surface at 1.30 , 1.55 and 1.70 GHz, are shown in Figures 16 (a), (b), and (c) respectively. Figure 16 displays the current distributions on the surfaces of the bottom of the filter structure, with the responses depicted in Figure 15, in the lower stopband, in the passband, in the upper stopband. Figures 16 (a) and (c) imply that no coupling takes place between the resonators in the lower stopband and the upper stopband. However, the high current densities shown in Figure 16 (b) reveal the strong coupling causing the required resonance. It is clear that most of the resonator length contribute to resonance. A prototype of the proposed 2nd iteration fractal DGS BPF with $W=1.5$ mm, $X=5.0$ mm and $D=1.0$ mm has been fabricated using the same substrate as shown in Figure 17.

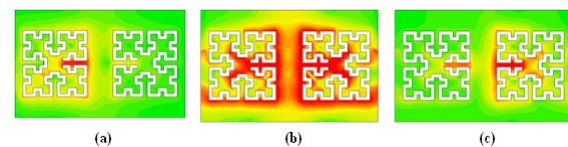


Figure 16. The current distributions on the surface of the ground plane of the filter with responses depicted in Figure 15 at (a) 1.3 GHz, (b) 1.55 GHz, and (c) 1.7 GHz.

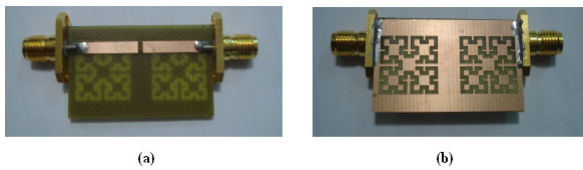


Figure 17. Photos of the fabricated prototype of the proposed 2nd iteration fractal DGS BPF with $W=1.5$ mm, $X=5.0$ mm and $D=1.0$ mm; (a) The top view and (b) The bottom view.

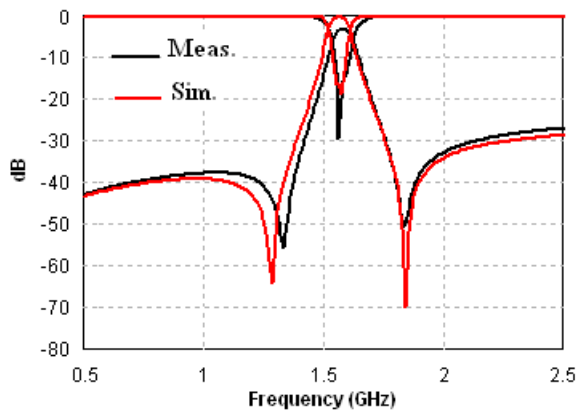


Figure 18. Measured and simulated return loss and transmission responses of the fabricated filter prototype depicted in Figure 17.

A prototype of the proposed 2nd iteration fractal DGS BPF with $W=1.5$ mm, $X=5.0$ mm and $D=1.0$ mm has been fabricated using the same substrate as demonstrated in Figure 17. Figure 18 illustrates the measured and simulated reflection coefficient and transmission responses of the fabricated filter prototype. Measured results of a fabricated prototype of a 2nd iteration fractal DGS BPF have shown reasonable agreement with those predicted by simulation. There is a slight shift of the lower edge of the passband response of the transmission characteristics, while the upper edge is very close. Besides, measured results show attenuation in the passband. The differences between the measured and simulated results are attributed to the fabrication tolerances; more advanced production technique together with a substrate with precise specifications will lead to results with higher agreement.

A comparison among the performance of the BPFs presented in this paper and with that reported in most recently published work²⁷ is summarized in Table 1. Even though the additive size reduction of the 2nd iteration fractal DGS BPF is small but this filter offers the best

selectivity in terms of the lower and the upper edges roll-off rates. The areas occupied by each filter have been expressed in terms of λ_g^2 calculated at the center frequency corresponding to each filter. Although the DGS BPF presented in²⁸ is almost comparable in size with proposed one, but it has poor upper edge roll-off rate and low selectivity in the lower edge roll-off rate.

Table 1. Comparison of the presented DGS BPFs with some published work

Filter Type	Filter size λ_g^2	Roll-off Rate (lower edge) dB/GHz	Roll-off Rate (upper edge) dB/GHz
Zero iteration DGS	0.45×0.23	78.51	47.10
1st iteration DGS	0.30×0.15	132.74	94.81
2nd iteration DGS	0.29×0.14	197.70	180.04
DGS BPF ²⁷	0.50×0.25	72.54	52.86
DGS BPF ²⁸	0.22×0.17	41.11	12.75

6. Conclusions

A Minkowski fractal based DGS resonator presented in this paper has proved its validity to design miniaturized microstrip BPFs. In addition to the reasonable performance of the proposed filter, the application of Minkowski fractal based DGS resonator results in filter structures with more compact size reduction in comparison with those reported in the literature. Results have revealed that further filter miniaturization might result in when applying higher fractal levels. In practice, this might not be satisfied for all iteration levels because there are many limitations encountered to production of the filter prototype. The results have shown that the filter performance has shown a low loss in the passband and high rejection in the stopband with considerable reduction of higher harmonics. Most important, the resulting filter has high selectivity with steep roll-off rates at both the lower and the upper edges of the passband. A prototype of a 2nd iteration fractal DGS BPF has been fabricated. Measured results of a have shown reasonable agreement with those predicted by simulation. The proposed filter performance, together with the extra size reduction; makes it suitable a candidate for use in a wide variety of recently available wireless services.

7. Acknowledgement

This work is supported by the Directorate of Research and Development in MOHESR, Iraq. The authors would like to thanks to the staff of the Electronics Design Center, especially to Ghaleb N. Radad, Mahmood R. Muhsen and Ahmed J. Qasim from Ministry of Science and Technology, Iraq, for their support in the production and measurements of the presented filter prototype.

8. References

1. Cohen N. Fractal antenna and fractal resonator primer. Chapter 8, In: Rock JA, van Frankenhuijsen M, editors. *Fractals and Dynamics in mathematics, science, and the arts: Theory and applications*, Volume 1, World Scientific Publishing; 2015.
2. Ali JK, Ahmed ES. A new fractal based printed slot antenna for dual band wireless communication applications. *Proceedings of Progress in Electromagnetics Research Symposium, PIERS 2012, Kuala Lumpur: Malaysia*; 2012 Mar; p. 1518–21.
3. Ali JK, Jalal ASA. A miniaturized multiband Minkowski-like pre-fractal patch antenna for GPS and 3g IMT-2000 Handsets. *Asian Journal of Information Technology*. 2007 May; 6(5):584–8.
4. Ali JK, Yassen MT, HussanMR, Salim AJ. A printed fractal based slot antenna for multi-band wireless communication applications. *Proceedings of Progress in Electromagnetics Research Symposium, PIERS 2012, Moscow: Russia*; 2012 Aug. p. 618–22.
5. Mezaal YS. New compact microstrip patch antennas: design and simulation results. *Indian Journal of Science and Technology*. 2016 Mar; 9(12). DOI: 10.17485/ijst/2016/v9i12/85950.
6. Abdulkarim SF, Salim AJ, Ali JK, Hammoodi AI, Yassen MT, Hussan MR. A compact Peano-type fractal based printed slot antenna for dual-band wireless applications. *2013 IEEE International RF and Microwave Conference, RFM 2013, Penang: Malaysia*; 2013 Dec. p. 329–32.
7. Ali JK, AL-Hussain ZAA, Osman AA, Salim AJ. A new compact size fractal based microstrip slot antenna for GPS applications. *Proceedings of Progress in Electromagnetics Research Symposium, PIERS 2012, Kuala Lumpur: Malaysia*; 2012 Mar. p. 700–3.
8. Ali JK, Abdulkareem SF, Hammoodi AI, Salim AJ, Yassen MT, Hussan MR, Al-Rizzo H. Cantor fractal based printed slot antenna for dual band wireless applications. *International Journal of Microwave and Wireless Technologies*. 2016 Mar; 8(02):263–70.
9. Ghiyasvand M, Bakhtiari A, Sadeghzadeh RA. Novel microstrip patch antenna to use in 2x2 sub arrays for DBS reception. *Indian Journal of Science and Technology*. 2012 Jul; 5(7). DOI: 10.17485/ijst/2012/v5i7/30493.
10. Ye CS, Su YK, Weng MH, Wu HW. Resonant properties of the Sierpinski-based fractal resonator and its application on low-loss miniaturized dual-mode bandpass filter. *Microwave and Optical Technology Letters*. 2009 May; 51:1358–61.
11. Weng MH, Jang LS, Chen WY. A Sierpinski-based resonator applied for low loss and miniaturized bandpass filters. *Microwave and Optical Technology Letters*. 2009 Feb; 51(2):411–13.
12. Mezaal YS, Eyyuboglu HT, Ali JK. New microstrip bandpass filter designs based on stepped impedance Hilbert fractal resonators. *IETE Journal of Research*. 2014 Jul; 60(3):257–64.
13. Mezaal YS, Ali JK, Eyyuboglu HT. Miniaturised microstrip bandpass filters based on Moore fractal geometry. *International Journal of Electronics*. 2015 Aug; 102(8):1306–19.
14. Ali JK, Miz'el YS. A new miniature Peano fractal-based bandpass filter design with 2nd harmonic suppression. *Proceedings of 3rd IEEE International Symposium on Microwave, Antenna, Propagation and EMC Technologies for Wireless Communications, Beijing: China*. 2009 Oct. p. 1019–22.
15. Ali JK, Mezaal YS. A new miniature narrowband microstrip bandpass filter design based on Peano fractal geometry. *Iraqi Journal of Applied Physics*. 2009 Dec; 5(4):3–9.
16. Ali JK, Alsaedi H, Hasan MF, Hammas HA. A peano fractal-based dual-mode microstrip bandpass filters for wireless communication systems. *Proceedings of Progress in Electromagnetics Research Symposium, PIERS; Moscow: Russia*. 2012 Aug. p. 888–92.
17. Mezaal YS, Eyyuboglu HT, Ali JK. A new design of dual band microstrip bandpass filter based on Peano fractal geometry: Design and simulation results. *Proceedings of the 13th IEEE Mediterranean Microwave Symposium, MMS'2013, Saida: Lebanon*. 2013 Sep. p. 1–4.
18. Ali JK. A new miniaturized fractal bandpass filter based on dual-mode microstrip square ring resonator. *Proceedings of the 5th International Multi-Conference on Signals, Systems and Devices, IEEE SSD '08, Amman: Jordan*; 2008 Jul. p. 1–5.
19. Ali JK, Hussain NN. A new fractal microstrip bandpass filter design based on dual-mode square ring resonator for wireless communication systems. *Iraqi Journal of Applied Physics*. 2009 Mar; 5(1):7–14.
20. Ali JK, Hussain NN. An extra reduced size dual-mode bandpass filter for wireless communication systems. *Proceedings of Progress in Electromagnetics Research Symposium, PIERS 2011, Suzhou, China*. 2011 Sep. p. 1467–70.
21. Liu JC, Liu HH, Yeh KD, Liu CY, Zeng BH, Chen CC. Miniaturized dual-mode resonators with Minkowski-island-based fractal patch for WLAN dual-band systems. *Progress in Electromagnetics Research C*. 2012; 26:229–43.
22. Lalbakhsh A, Neyestanak AAL, Naser-Moghaddasi M. Microstrip hairpin bandpass filter using modified Minkowski fractal-shape for suppression of second harmonic. *IEICE Transactions on Electronics*. 2012 Mar; E95C(3):378–81.

23. Chen J, Weng ZB, Jiao YC, Zhang FS. Lowpass filter design of Hilbert curve ring defected ground structure. *Progress in Electromagnetics Research*. 2007; 70:269–80.
24. Liu HW, Li ZF, Sun XW. A novel fractal defected ground structure and its application to the low-pass filter. *Micro-wave and Optical Technology Letters*. 2003 Dec; 39:453–6.
25. Alqaisy M, Chakraborty C, Ali JK, Alhawari ARH. A miniature fractal-based dual-mode dual-band microstrip band-pass filter design. *International Journal of Microwave and Wireless Technologies*. 2015 Apr; 7:127–33.
26. Li TP, Wang GM, Lu K, Xu HX, Liao ZH, Zong B. Novel bandpass filter based on CSRR using Koch fractal curve. *Progress in Electromagnetics Research Letters*. 2012; 28:121–8.
27. Boutejdar A, Ibrahim AA, Burte EP. DGS resonators form compact filters. *Microwaves and RF*. 2015 Mar; 54(3):52–60.
28. Boutejdar A, Elsherbini A, Balalem A, Machac J, Omar A. Design of new DGS hairpin microstrip bandpass filter using coupling matrix method. *Proceedings of Progress in Electromagnetics Research Symposium, PIERS 2007, Prague: Czech Republic*. 2007 Aug. p. 261–5.
29. IE3D User's Manual, Release 12.3. Zeland Software, Inc., Fremont, CA; 2007.
30. Hong JS. *Microstrip Filters for RF/Microwave Application*. New York, Wiley; 2001.
31. Srikanth S, Jeyalakshmi V. Compact UWB micro strip band pass filter with open circuited stubs. *Indian Journal of Science and Technology*. 2015 Jul; 8(13). DOI: 10.17485/ijst/2015/v8i13/58531.
32. Wang J, Xu LJ, Zhao S, Guo YX, Wu W. Compact quasi-elliptic microstrip lowpass filter with wide stopband. *Electronics Letters*. 2010 Sep; 46(20):1384–5.
33. Li JL, Qu SW, Xue Q. Compact microstrip lowpass filter with sharp roll-off and wide stop-band. *Electronics Letters*. 2009 Jan; 45(2):110–11.
34. Hayati M, Naderi S, Jafari F. Compact microstrip lowpass filter with sharp roll-off using radial resonator. *Electronics Letters*. 2014 May; 50(10):761–2.